Cement & Concrete Composites 31 (2009) 171–175

Contents lists available at ScienceDirect

Cement & Concrete Composites

journal homepage: www.elsevier.com/locate/cemconcomp

Milli X-ray fluorescence X-ray spectrum imaging for measuring potassium ion intrusion into concrete samples

Jeffrey M. Davis [a,*], Dale E. Newbury [a], Prasada rao Rangaraju [b], Senthil Soundrapanian [b], Colin Giebson [c]

[a] National Institute of Standards and Technology, Microanalysis Research Group, 100 Bureau Drive, Mail Stop 8371, Gaithersburg, MD 20899, United States
[b] Department of Civil Engineering, Clemson University, 109 Lowry Hall, Clemson SC 29631, United States
[c] Finger Institut fuer Baustoffkunde, Bauhaus-Universitaet Weimar, Coudraystrasse 11, 99421 Weimar, Germany

ARTICLE INFO

Article history:
Received 14 May 2008
Received in revised form 10 December 2008
Accepted 12 December 2008
Available online 25 December 2008

ABSTRACT

Of particular interest when studying the effects of deicing solutions on concrete is the depth of penetration of ions from deicing salts. To determine the limits of positive ion infiltration, a method based on milli X-ray fluorescence (mXRF) has been developed. This method combines traditional energy dispersive spectrometry (EDS) with stage movement X-ray mapping to analyze comparatively large areas of concrete. The result is the ability to determine the depth of ion infiltration over a distance of tens of millimeters. The technique also requires minimal preparation of the sample, and due to the nature of the X-ray beam, concrete samples do not have to be coated to reduce charging. This paper describes in detail the method of mXRF with X-ray spectrum imaging (XSI) for concrete applications and shows two examples where potassium ion infiltration was measured with mXRF-XSI as part of broader studies in pavement durability.

Published by Elsevier Ltd.

1. Introduction

X-ray fluorescence (XRF) is a well established elemental analysis technique based upon excitation of a specimen with a primary beam of characteristic and/or continuum X-rays derived from an electron beam excited metal target [1]. Photoelectric absorption of the primary X-rays by specimen atoms results in inner shell ionization that leads to emission of characteristic X-rays. Measurement of the energies of these secondary X-rays by energy dispersive X-ray spectrometry identifies the elemental species present in the excited volume, and the characteristic intensities referenced to standards of similar composition can provide elemental mass concentrations, typically to ±10% relative standard deviation or better. XRF is traditionally regarded as a bulk analysis method because the primary beam has dimensions of millimeters to centimeters and the depth of penetration of the primary radiation is typically tens of micrometers depending on the composition of the target. Milli X-ray fluorescence (mXRF) employs a capillary X-ray optic that focuses the X-ray beam into a spot nominally 40 μm in diameter [2]. Elemental mapping is achieved by step scanning a large (100 cm^2), precision (step motor reproducibility of approximately ±10 μm) mechanical stage to generate a user-defined grid of beam locations. To maximize the collection of analytical information, the method of X-ray spectrum imaging (XSI) is employed, in which the entire EDS spectrum is recorded at each beam location. This procedure results in the collection of a "data cube", a hyperspectral database whose individual members consist of information encoded as $[x,y,I(E)]$. In the database, x and y represent the stage location and $I(E)$ is the EDS spectrum, typically recorded as 2048 channels of 10 eV width, with a maximum intensity of 16-bits (65 535 counts) per channel. Efficient software tools such as NIST-Lispix have been developed to "mine" these large (100 MB or greater) databases to recover elemental maps [3].

The X-ray beam size and the large specimen area accessible with the mechanical stage of mXRF makes it unusual among the broad suite of microanalytical tools, which include electron beam induced X-ray emission in the scanning electron microscope (SEM) and various optical spectrometries performed in optical microscopes. These methods operate at the micrometer to nanometer lateral spatial scale, and more importantly, are limited in their lateral view of the specimen to regions generally less than 10 mm in linear dimensions. These microanalytical techniques can be used to map larger areas if the specimen chamber and mechanical stage will permit sufficient motion, but large area mapping requires tiling large numbers of small area maps. The 40 μm beam of mXRF combined with mechanical stepping of a large precision stage is ideally suited to study materials that vary on the millimeter to centimeter scale. Concrete, composed of cement paste, sand, coarse aggregate and water, is a material that varies on the macroscopic scale as well as the millimeter, micrometer and nanometer scale. When considering the impact of deicing solutions on concrete and their penetration, chemical gradients that develop on the millimeter scale are very important, and mXRF-XSI is a highly effective tool for characterization.

* Corresponding author. Tel.: +1 301 975 6988.
E-mail address: Jeff.davis@nist.gov (J.M. Davis).

0958-9465/$ - see front matter Published by Elsevier Ltd.
doi:10.1016/j.cemconcomp.2008.12.005

Deicing solutions are applied to pavements frequently during winter months to melt ice or prevent snow from accumulating on pavements. Traditional salts such as sodium chloride (as mineral halite) and urea have detrimental effects on both concrete and the environment [4]. In particular, a well known mechanism of chloride ion infiltration in concrete is blamed for the corrosion of reinforcing steel in bridge decks [5]. Alkali-containing deicers based on the salts of acetates and formates have been used since the early 1990s for winter maintenance on airfield concrete pavements. In recent years, severe distress occurred on airfield concrete pavements (such as those identified in the United States [6] and Germany [7]) due to deleterious alkali–silica reactions (ASR). Investigations showed that externally supplied alkalis are capable of favoring ASR in concretes with alkali-reactive aggregates. Research showed that acetate and formate based deicers showed a highly accelerative effect on ASR [8].

The focus this paper is to show a technique for measuring the concentration of potassium in a concrete matrix. Researchers at Clemson and in Weimar, Germany were interested in the depth of penetration of externally supplied potassium, as both groups were testing the effects of potassium based deicing solutions on concrete pavements. At Clemson, the concrete was prepared according to the ASTM C672 specifications with slight modification for testing potassium acetate. The concrete prisms from Weimar were prepared with a new ASR performance-test that is designed to assess real job mixtures under the influence of deicing solutions [9] through a cyclic process of deicer application, ponding, freezing and drying the prisms. During the course of the research, both groups expressed a need to determine the depth of infiltration of potassium into the sample, and to determine the concentration or concentration gradient of potassium within the sample. While this paper will not comment on the relative impact of each of the deicing solutions on the durability of concrete, in this paper, we will report the method used to determine the depth of penetration of potassium ions.

One alternative method to determine the depth of potassium ion infiltration, proposed by Livingston et al. employs the technique of autoradiography [10]. Using the natural radiation produced by potassium, a photographic plate can be exposed to a large section of concrete in situ. Given the possibility for large area analysis, autoradiography is faster than mXRF. The mXRF technique gains its advantage in the ability to determine the concentrations of all the major elements present in concrete, not just potassium ions. These include calcium, silicon, sulfur and iron, among others. The method gains power in hyperspectral analysis as well. Because full spectra are recorded at each point, a variety of multivariate analyses can be performed in order to determine the phases present in the concrete [11]. In addition, because of the small probe size, the cement can be analyzed independently of the aggregate. The large beam size in conventional XRF makes analysis of hardened concrete difficult to quantify and relate to known cement and concrete mineral phases. Finally, the mXRF unit moves the stage under the X-ray beam, rather than rastering the beam as in electron microprobe instruments, so as to allow very large areas to be mapped.

2. Experimental method

In this study, samples of concrete were cast using well known and characterized cements and aggregates. Commercial grade deicing solutions (50% mass fraction potassium acetate or 50% mass fraction potassium formate) were applied on the top surface of the concrete for 3 months at Clemson, and 6 months at Weimar. Subsequently, the concrete samples were cored and sectioned in preparation for analysis. All concrete samples were depth cross-sectioned in order to show the top and bottom surfaces of the concrete in the same plane. Samples from Clemson were sectioned to measure approximately 30 mm by 35 mm, and were mounted in epoxy in order to polish the surface. The depth into the pavement on the Clemson samples is measured on the vertical axis. Samples from Weimar were approximately 100 mm by 30 mm and were polished at NIST using silicon carbide grinding papers.

The Eagle III micro-XRF unit[1] used for the experiments presented here is equipped with an EDAX 30 mm^2 Si(Li) Energy Dispersive Spectrometer (EDS). It operates in both ambient air pressure and under low vacuum. The low vacuum is useful for detecting aluminum, silicon and sulfur, as these X-rays are strongly absorbed along the air path to the EDS. It should be noted, however, that because the primary element of interest was potassium, the entire experiment could have been run at ambient air pressure. However, when quantification is desired, it is necessary to account for silicon because it represents a significant portion of both the aggregates and the cement paste; so a vacuum path was utilized for these measurements.

For quantification, a series of well characterized NIST glasses including NIST SRM 470 were used as standards. The glasses were chosen to provide reference intensities for aluminum, silicon, potassium, calcium and iron in a matrix similar to the cement compound, thus minimizing matrix corrections necessary for quantification. The quantification procedure provided in the EDAX mXRF analytical software follows the fundamental parameters approach with the addition of empirical standards [12,13]. The standards analysis indicated that, using the same operating conditions for the standard and experimental analysis, the results could be quantified to approximately plus or minus 5% relative standard deviation. Throughout the experiment, the excitation energy was held constant at 20 keV through the rhodium source, and tube currents were adjusted such that the pulse processor had approximately 30% dead time.

The beam size and the resulting lateral sampling area were measured directly. A tungsten wire approximately 50 μm in diameter was suspended in air and the stage was moved such that the beam scanned over it. By taking the full width of the integrated tungsten peak intensity at half the maximum value of the peak, the width of the beam was determined to be 43 μm in diameter.

To determine the lateral sampling area, a small piece of copper was pressed up against a flat polished section of concrete. The result was an abrupt interface between the copper and concrete with no intermediate phase. By scanning the beam across this abrupt interface, the width of the area where the copper interface could be detected at a signal level of 5% of the full copper intensity while the beam was placed in the concrete is defined as the lateral sampling area. While the method is not exact, the purpose of measuring the lateral sampling area is to determine the proper strategy for selecting the number and effective size of the mapping pixels. Slight oversampling (i.e., pixels overlap) is desirable, but the time penalty for extensive oversampling is severe, so choosing a careful mapping strategy is important. Using this method, the lateral sampling area was determined to be approximately 160 μm in diameter.

Taking into consideration the lateral sampling area, the next step is to determine the pixel density of the X-ray maps. Because an X-ray map is essentially a collection of thousands of consecutive points, the pixel density translates into the number of points analyzed across the sample. One might assume that the pixel density should simply be the ratio of the specimen area to the lateral sampling area. Such an assumption, however, assumes a uniform signal

[1] Commercial equipment, instruments, and materials, or software are identified in this report to specify adequately the experimental procedure. Such identification does not imply recommendation or endorsement of these items by the NIST, nor does it imply that they are the best available for the purpose.

density from the entire beam interaction region. Like the beam itself, the signal density, defined as the relative number of X-rays created by the sample given its distance from the incident beam center, follows a roughly Gaussian distribution. Thus, the signal at the edges of the interaction volume is comparatively weak to that in the center. Ultimately, the most important factor in pixel density calculations is time. It should be noted, however, that higher pixel density does not necessarily translate into higher image or data quality. X-ray images of concrete are composed of numerous interface pixels between the aggregate and the cement paste. Such interfaces will exist wherever the X-ray beam is capable of fluorescing both the aggregate and the cement paste, and these pixels at the interface will not conform to any known cement or mineralogical phase. Increasing the number of pixels in an effort to provide higher spatial resolution is likely to simply generate more interface pixels. For the purpose of concrete X-ray mapping, a value of 80 μm per pixel was used. This represents approximately twice the nominal beam diameter, and approximately half the lateral sampling area.

3. Results

The first set of concrete analyzed was from Clemson University. Potassium ions penetrated approximately 15 mm into the sample. This was evident from viewing the potassium X-ray image shown as Fig. 1. The brightest pixels at the top of the image indicate the region of the highest potassium concentration. As the potassium concentration decreases deeper in the sample, the pixels also decrease in brightness. This sample was the best example of the unique gradient nature of potassium ion infiltration. In order to analyze the gradient seen in the concrete sample, a method was developed within Lispix that allowed the analyst to analyze infil-

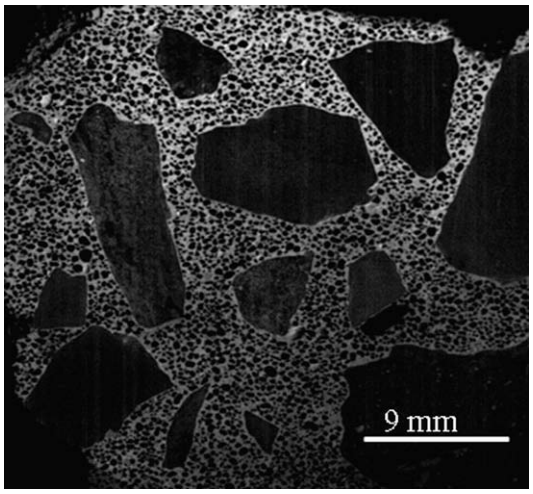

Fig. 1. The potassium X-ray map from the Clemson University sample. The concrete was treated with potassium acetate deicing solutions by ponding on the exposed surface, shown as the top of the X-ray map. The gradient of concentration from top to bottom, as represented by pixel brightness.

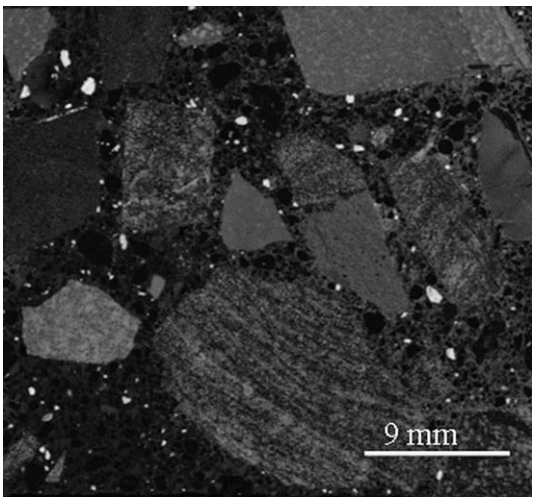

Fig. 3. The potassium X-ray map from the control Weimar University sample. The concrete was made using greywacke stone which has potassium bearing mineral phases. This control sample was not treated with deicing salts.

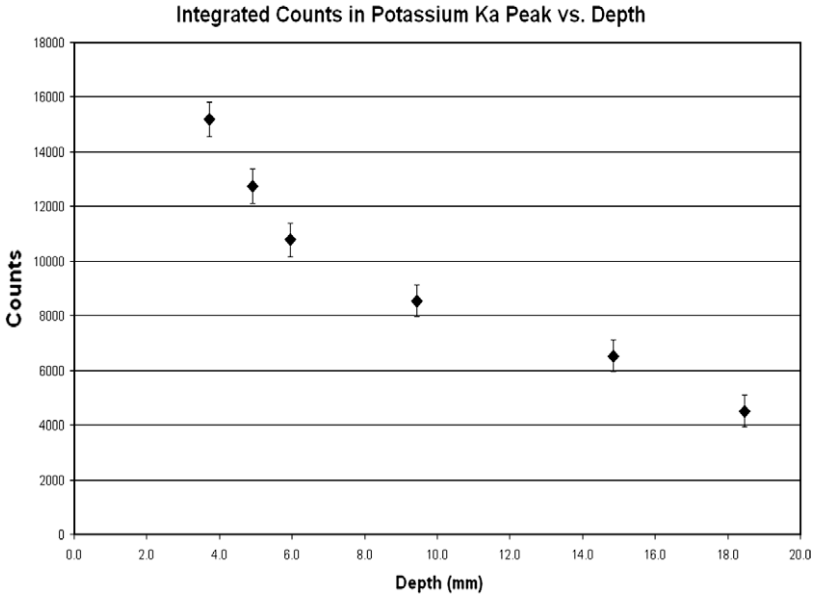

Fig. 2. Chart showing the relationship between potassium concentration and depth in the concrete sample shown in Fig. 1. The *x*-axis represents depth as measured from the top of the image, and the *y*-axis represents the integrated counts in the potassium peak. Error bars represent standard deviation of repeat measurements for the value of total counts in the potassium K-alpha peak.

tration based on the centroid of a series of pixel thresholds. According to the process, a series of six brightness thresholds called "bins" were defined. The bins did not overlap brightness values, and each bin represented thirty gray-scale values (full gray-scale on the image was 256 values). Each successive bin, starting with the brightest, contained a group of pixels deeper in the sample. After each bin was defined, a binary mask of the pixels in the bin was generated. The binary mask was used to derive an X-ray spectrum. As each spectrum was derived, the integrated counts in the potassium K-alpha peak were calculated and the final result was plotted against the *y*-centroid. The *y*-centroid represented the average depth of penetration of the potassium ions in the mask of the particular bin. This result is shown as Fig. 2.

Samples from Weimar were considerably more difficult to analyze. First, the cement paste itself had slightly higher potassium concentrations than the Clemson concrete. This is largely because the Clemson concrete was specifically selected as a low alkali cement, while the Weimar cement is a more common, higher alkali cement. In addition, the concrete was made from aggregates that had naturally occurring potassium rich phases. Figs. 3 and 4 show part of the Weimar concrete sample. The Weimar samples were particularly striking because of the incredible distance through which the potassium ions had penetrated. Shown in Fig. 3, the cement paste between aggregates has very little cement because the sample was not treated with deicing salts. Fig. 4, however, shows considerably higher potassium concentration, despite both samples being made with the same cement. As prepared, the Weimar samples represented approximately 100 mm of depth in the concrete sample. The potassium ions appear to have penetrated the entire length of the sample.

The intermingling potassium phases in the Weimar concrete made it necessary to phase map the area. Phase mapping, accord-

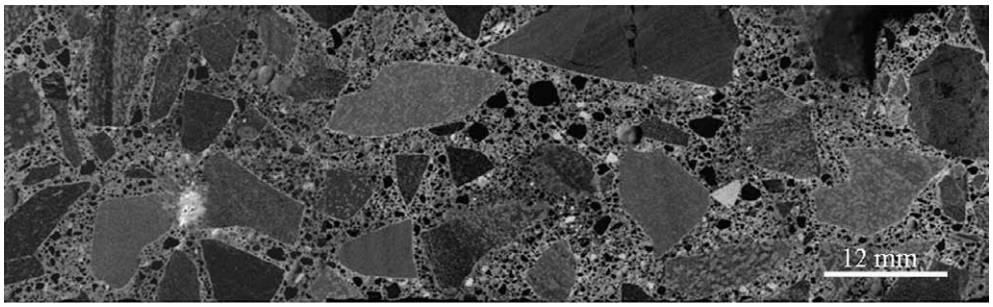

Fig. 4. The potassium X-ray map from the experimental Weimar University sample. This concrete sample was treated with potassium formate deicing solution. The top surface of the concrete is on the left side of the image, while the bottom surface is on the right. The expected migration of ions in the sample was from left to right. However, the potassium ions appear to have traveled through the entire cement paste.

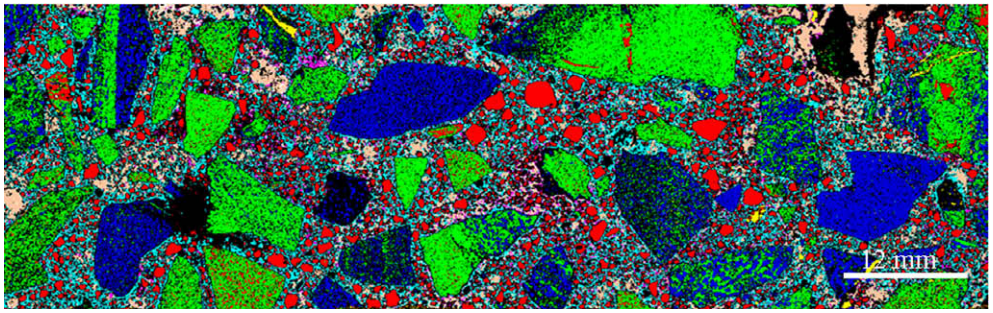

Fig. 5. Colorized X-ray phase map of Weimar concrete sample. The phases represented here are assigned to a series of colors. Red pixels are assigned to silicon dioxide, green and blue pixels are assigned to graywacke stone, light blue phases are assigned to the potassium silicate phase, and orange pixels are assigned to a unique calcium rich ettringite phase. The full width of this image is 96 mm representing 96 mm of depth in the concrete. The left side of the image is the top of the concrete surface where the deicing solutions were applied. (For interpretation of the references in colour in this figure legend, the reader is referred to the web version of this article.)

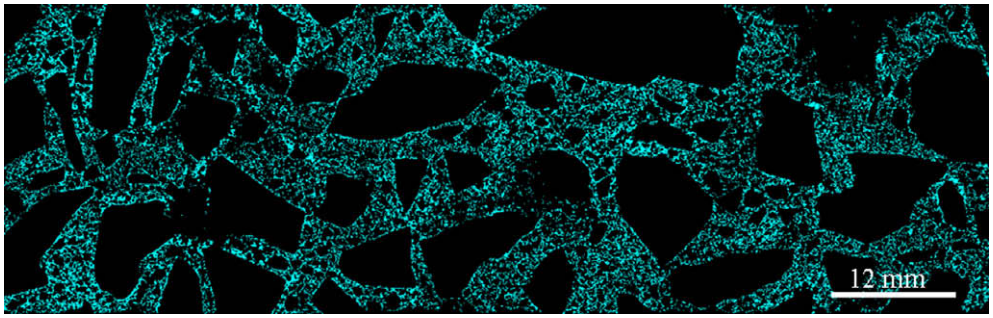

Fig. 6. Binary map of Weimar sample showing only pixels assigned to the potassium rich phase.

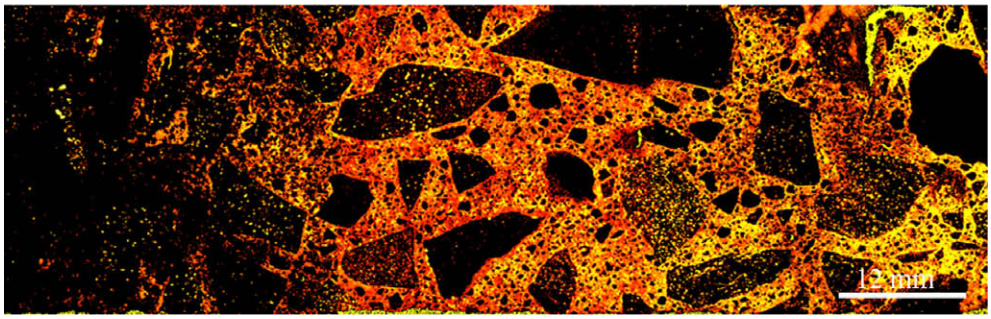

Fig. 7. Elemental X-ray map of sulfur concentration in the Weimar concrete sample. Sulfur oxide concentrations range from below 1% sulfur oxide (black) to greater than 3% sulfur oxide (white). At the top surface of the concrete, as shown on the left side of the image, the concentration for sulfur is very low.

ing to the NIST-Lispix method, assigns phases to pixels in an X-ray image based on the composition of that pixel. For instance, a pixel whose composition is 70% calcium oxide and 20% silicon oxide (mass fraction) will be assigned to a calcium silicon hydrate phase representing cement paste. For the purpose of this experiment, the potassium was assigned to either a potassium bearing aggregate or to the potassium in the cement paste based on the composition of other elements in the pixel. Seen in Fig. 5, the pixels colored in light blue represent a potassium rich calcium silicon hydrate phase. Fig. 6 shows only those pixels from the potassium rich phase. Specifically, the potassium concentration ranged from 7% to 11% (mass fraction) potassium oxide. This potassium rich cement paste extends across the entire length of the sample, yet it is almost completely absent from the control sample seen in Fig. 3.

Taking advantage of the full analytical capability of EDS X-ray Spectrum Imaging, the sulfur X-ray maps were also extracted from the data cubes. Interestingly, the first 20 mm of the sample appear to have very little sulfur as shown in Fig. 7. Unlike radiographic techniques, the X-ray fluorescence technique has the ability to analyze all of the elements in the sample, including the non-radioactive ones such as sulfur. A future publication will consider in detail the full chemistry of these complex microstructures and interactions, and will likely employ a full multivariate statistical analysis on the hyperspectral data in order to fully identify and quantify the phases present.

4. Summary and conclusions

Studying the long term effects of ion infiltration into concrete, especially where pavement durability is concerned, presents a number of measurement challenges. First, gradients of concentration due to the infiltration of ions such as chlorine and potassium tend to occur over centimeters along the axis of depth. This naturally precludes many microscopy techniques, such as electron probe microanalysis, from consideration, because their limited sampling area is unable to show the full scale of the gradient. The mXRF technique, through stage scanning and a mid-range beam size is able to show infiltration gradients over centimeters without the need for extensive tiling or under-sampling. Second, the interactions of compounds and ions provided by deicing solutions in concrete are complex, and the secondary reactions are not well understood. Stains and other analysis techniques that are element specific will provide information about one element in the sample, but not about all of the elements of interest. Analysis of X-ray spectrum images gives the analyst the ability to analyze all of the elements present in the system, and most importantly, to discover unexpected effects and possible correlations.

As debate continues over the effect of potassium ions on a concrete system, mXRF can provide answers to the depth of penetration question in addition to exploring the full range of reactions and secondary compounds formed as a result of potassium ion infiltration. Compared to autoradiography, mXRF methods still analyze comparatively small areas. It is likely that the system will be limited, in the short term, to well controlled laboratory tests done to establish an accepted rate for potassium ion infiltration. However, the system is not limited to potassium depth alone. Elements such as sulfur can also be analyzed in the system. As shown in this paper, the sulfur concentration across the Weimar concrete sample showed a complex gradient from low concentrations at the top surface to high concentrations at the bottom. The hyperspectral nature of the data allows analysts to compare a series of elemental maps and to identify phases present. With more research on a wider field of materials, this new method will provide unique insights into what happens to concrete when exposed to deicing salts. In terms of broader applications, the mXRF method also shows promise for analyzing many other materials, as well as for a number of concrete durability related issues.

References

[1] Hevesy G. Chemical analysis by X-ray spectroscopic methods and its applications. New York: McGraw-Hill; 1932. p. 333.
[2] Rindby A, Engstrom P, Larsson S, Stocklassa B. Microbeam technique for energy-dispersive X-ray fluorescence. X-ray Spectrom 1989:109–12.
[3] Bright DB. LISPIX: image processing and data visualization tool for the PC and Macintosh. Scanning 2000;22(2):111–2.
[4] Amrhein C, Strong JE. The effect of deicing chemicals on major ion and trace metal chemistry in roadside soil. In: Proceedings of the environmental impact of highway deicing, UC-Davis; 1989.
[5] ACI Committee 222. Corrosion of metals in concrete. Farmington Hills (MI): American Concrete Institute; 1997 [ACI 222R-96].
[6] Rangaraju PR, Olek J. Potential for acceleration of ASR in the presence of pavement deicing chemicals. Final Report, IPRF-01-G-002-03-9; February 2007. p. 127.
[7] Stark J, Freyburg E, Seyfarth K, Giebson C. Latest insights and advances in understanding the ASR and state-of-the-art ASR-test methods in Germany. Int J Restorat Build Monum (IJRBM), Aedificatio Verlag GmbH Freiburg 2006;12(5/6):371–86.
[8] Stark J, Bellmann F, Gathemann B, Seyfarth K, Giebson C. The influence of alkali-containing deicing agents on the alkali–silica reaction in pavement concretes for roads and airports. ZKG Int 2006;59(11):74–82.
[9] Stark J, Giebson C. Assessing the durability of concrete regarding ASR. In: Proceedings of the 7th CANMET/ACI international conference on durability of concrete, Montreal, Canada; 2006. p. 225–38 .
[10] Livingston RA, Aderhold HC, Hover KC, Hobbs SV, Cheng YT. Autoradiographic methods for identifying alkali–silica reaction gel. ASTM J Cem Concr Aggr 2000;22(1).
[11] Kotula PG, Keenan MR, Michael JR. Automated analysis of SEM X-ray spectral images: a powerful new microanalysis tool. Microsc Microanal 2003;9:1–17.
[12] Sherman J. The theoretical derivation of fluorescent X-ray intensities from mixtures. Spectrochim Acta 1955;7:283–306.
[13] Criss JW, Birks LS, Gilfrich JV. Versatile X-ray analysis program combining fundamental parameters and empirical coefficients. Anal Chem 1978;50(1):33–7.